Clays and Clay Minerals, Vol. 37, No. 1, 29–40, 1989.

WEATHERING OF IRON-BEARING MINERALS IN SOILS AND SAPROLITE ON THE NORTH CAROLINA BLUE RIDGE FRONT: II. CLAY MINERALOGY

R. C. GRAHAM,[1,3] S. B. WEED,[1] L. H. BOWEN,[2]
D. D. AMARASIRIWARDENA,[2] AND S. W. BUOL[1]

[1] Department of Soil Science, North Carolina State University
Raleigh, North Carolina 27695

[2] Department of Chemistry, North Carolina State University
Raleigh, North Carolina 27695

Abstract—The mineralogy of the clay fraction was studied for soils and saprolite on two Blue Ridge Front mountain slopes. The clay fraction contained the weathering products of primary minerals in the mica gneiss and schist parent rocks. Gibbsite is most abundant in the saprolite and residual soil horizons, where only chemical weathering has been operable. In colluvial soil horizons, where both physical and chemical weathering have occurred, the clay fraction consists largely of comminuted primary phyllosilicates—muscovite, chlorite, and possibly biotite—and their weathering products: vermiculite, interstratified biotite/vermiculite (B/V), and kaolinite. The clay-size chlorite contains Fe^{2+}, as indicated by Mössbauer spectroscopy, and is more resistant to weathering than biotite. The vermiculite and B/V, both weathering products of biotite, contain Fe^{3+}. Vermiculite in colluvial soils and, especially, surface horizons is weakly hydroxy-interlayered. The kaolinite in the clay fraction resulted at least partly from the comminution of kaolinized biotite in coarser fractions.

The hematite content ranged from 0 to 8% of the clay fraction and strongly correlates (r = .95) with dry clay redness, as measured by the redness rating: RR = (10 − YR hue) × (chroma) ÷ (value). The hematite is largely a product of the weathering of almandine; thus, the soil redness is dependent on the amount of almandine in the parent materials and its degree of weathering in the soils. Goethite (13–22% of the clay fraction) imparts a yellow-brown hue to soils derived from almandine-free parent rocks. The release of Fe in relatively low concentrations during the weathering of Fe-bearing primary minerals, particularly biotite, appears to have promoted the formation of goethite.

Key Words—Chlorite, Goethite, Hematite, Iron, Kaolinite, Mössbauer spectroscopy, Saprolite, Soils, Vermiculite, Weathering.

INTRODUCTION

Gneisses and schists containing biotite and other Fe-bearing minerals are prevalent in the southeastern United States. Weathering of these rocks has produced secondary minerals, some of which are largely modifications of original mineral structures, e.g., biotite → vermiculite (Harris *et al.*, 1985; Rebertus *et al.*, 1986). Others have precipitated from solution in the soil, e.g., gibbsite and goethite (Calvert *et al.*, 1980; Schwertmann and Taylor, 1977).

Graham *et al.* (1989) described the weathering morphologies and associated alteration products of the sand-size primary minerals in soils and saprolite on the Blue Ridge Front and provided information on the sources of the secondary minerals. The clay-size fraction of the soils and saprolite contains the minerals most responsible for their chemical behavior, and in this paper the origin and characteristics of these minerals, particularly the Fe-bearing minerals, are reported.

MATERIALS AND METHODS

Soils were sampled on two Blue Ridge Front mountain slopes in Wilkes County, North Carolina. The slope positions and classifications of the sampled pedons are indicated in Table 1. The orientation of one slope coincides with the dip of the underlying foliated bedrock and is thus a "dip slope". Pedons DU, DE, and DH were sampled from the dip slope. The other slope is oriented transverse to the dip direction and is termed a "cross-dip slope". Pedons CS, CB, CL, and CF were sampled from the cross-dip slope. Pedon R was sampled from the ridge top between the two slopes. The physical setting of the study area is more completely described elsewhere (Graham, 1986). Characteristics of the mica gneiss and schist bedrock are reported by Graham *et al.* (1989).

Samples were collected from genetic soil horizons exposed by pits. The samples were air-dried and, after organic matter removal (Anderson, 1963), clays (<2 μm) were separated from the fine earth fraction (<2 mm) by sedimentation (Jackson, 1979). Na-saturated clay was dialyzed against distilled water until free of salt and freeze-dried. These clays were used for Möss-

[3] Present address: Department of Soil and Environmental Sciences, University of California, Riverside, California 92521.

Table 1. Classification of the pedons on the North Carolina Blue Ridge Front from which samples were obtained.

Pedon	Geomorphic position[1]	Family class	Subgroup
R	Ridge top	fine-loamy, oxidic, mesic	Typic Hapludult
CS	Shoulder, cross-dip slope	fine-loamy, micaceous, mesic	Typic Hapludult
CB	Cross-dip backslope	coarse-loamy, micaceous, mesic	Ruptic-Lithic-Entic Hapludult
CL	Lower cross-dip slope	fine-loamy, oxidic, mesic	Typic Hapludult
CF	Cross-dip footslope	coarse-loamy, oxidic, mesic	Typic Dystrochrept
DU	Upper dip slope	fine-loamy, micaceous, mesic	Typic Hapludult
DE	Dip slope escarpment	coarse-loamy, micaceous, mesic	Typic Dystrochrept
DH	Dip slope hollow	coarse-loamy, oxidic, mesic	Typic Dystrochrept

[1] Geomorphic relationships are more completely described in Graham (1986) and Graham *et al.* (1989).

bauer spectroscopy, citrate-dithionite extractions (Coffin, 1963), and differential thermal analysis (DTA). Mg- and K-saturated clay samples were smeared on glass slides for X-ray powder diffraction (XRD) (Theisen and Harward, 1962). Selected Na-saturated clays were treated with formamide to differentiate kaolinite and halloysite by intercalation (Churchman *et al.*, 1984). Instruments used for analyses and their operating conditions were described by Graham *et al.* (1989).

RESULTS

XRD analysis

All clay fractions analyzed by XRD produced a 10-Å mica peak when Mg saturated, but the specific identity of the mica could not be determined from the data for oriented clays in Figures 1–3. Both muscovite and biotite were identified in the parent rocks and in the soil sand fractions (Graham *et al.*, 1989) and may be present in the clay fractions. The relatively strong 5-Å 002 peak, somewhat less intense than the 10-Å 001 peak, indicated the presence of muscovite (Fanning and Kermidas, 1977), particularly in colluvial soil horizons, but did not rule out the presence of biotite.

Vermiculite is typically identified by a 14-Å peak which collapses to 10 Å on K-saturation of the sample (Jackson, 1979). In the present study, K-saturation and heating to 350°C accomplished only a partial collapse of the 14-Å mineral to about 10.7 Å in samples of the saprolite and soil horizons developed in residuum (Figures 1 and 2). Complete collapse to 10 Å was accomplished by heating the sample to 550°C. Collapse of the 14-Å peak was even less complete for samples from the colluvial soil horizons, particularly those near the soil surface (Figures 1–3). A broad peak at about 13 Å was produced by heating the sample to 350°C, and an 11-Å shoulder on the 10-Å peak resulted after heating the sample to 550°C. Hydroxy-interlayering of vermiculite is typically indicated by the incomplete collapse of the 14-Å (001) spacing toward 10 Å on K-saturating and heating the sample to 550°C (Barnhisel, 1977). The magnitude of this decrease in the 001 d-value provided an indication of the extent of the hydroxy-interlayering. If vermiculite interlayers contain large amounts of Al-hydroxy material, K-saturation and heating results in only small shifts in the 14-Å peak toward 10 Å (Barnhisel, 1977). The broad 11-Å shoulder produced by such treatment in the present study indicates that there was only minimal hydroxy-interlayering of the vermiculite.

All the soil clay fractions showed a rather broad XRD peak between 12 and 13 Å upon Mg-saturation (Figures 1–3), indicating an interstratified mica/vermiculite phase (Sawhney, 1977). In some traces, a 24-Å peak accompanied the 12-Å peak, suggesting a regular interstratification of 10- and 14-Å minerals (e.g., Figure 2, C horizon). A similar phase was noted in weathered, sand-size biotite grains by Graham *et al.* (1989). More often, no higher order peak was evident, and the interstratification was apparently random (Sawhney, 1977).

Primary chlorite is typically identified by the persistence of a 14-Å peak on heating the sample to 550°C (Barnhisel, 1977). Graham *et al.* (1989) found chlorite in both the schist and the gneiss parent rocks and in the soil sand fractions, but XRD traces presented in Figures 1–3 of the present study indicate that chlorite was present in clay fractions of only those soil horizons developed in colluvium.

The presence of kaolin-group minerals in the soil-clay fraction was indicated by a 7-Å peak which disappeared on heating the sample to 550°C (Figures 1–3) and confirmed by a DTA endotherm at about 550°C (data not shown). The formamide intercalation treatment described by Churchman *et al.* (1984) was used to distinguish kaolinite and halloysite. Only in saprolite (Cr horizon) clays was even a slight reduction of the 7-Å peak noted due to the expansion of halloysite (data not shown). Peak height changes in B-horizon clays were very small and inconclusive. Apparently, kaolinite was the dominant kaolin-group mineral in these soils, although small amounts of halloysite were identified in Cr horizons.

Gibbsite, identified by peaks at about 4.85 and 4.37 Å that disappeared on heating the sample to 350°C (Jackson, 1979), showed intense peaks in the clay fraction of saprolite and soil horizons developed in resid-

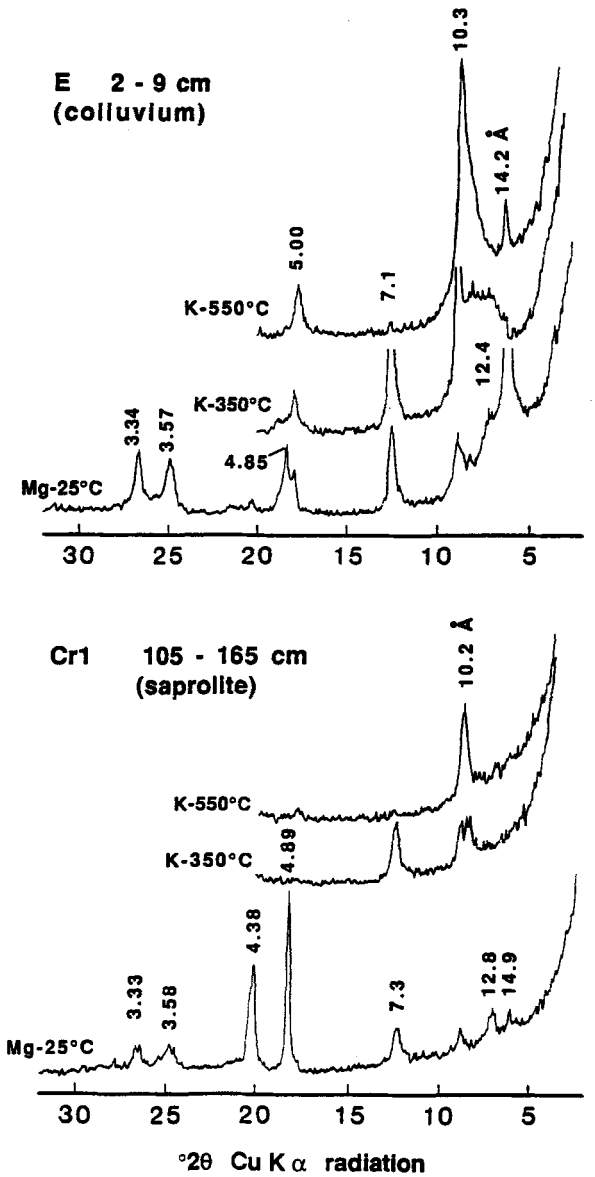

Figure 1. X-ray powder diffraction patterns for the <2-μm fraction of selected horizons from Pedon CL. (a) The E horizon has been chemically and physically weathered, (b) the Cr1 horizon has been only chemically weathered.

uum (Figures 1 and 2). In colluvial soil horizons, the intensity of the gibbsite peaks was much reduced relative to the phyllosilicate peaks (Figures 1–3).

Goethite was identified in some samples by a small, broad peak at about 4.18 Å (e.g., Figure 2).

Mössbauer analysis

Figure 4 illustrates typical Mössbauer spectra for the clays. Representative Mössbauer data are compiled in Tables 2 and 3.

The 298-K spectrum for the Pedon CF Bt1 horizon (Figure 4a) shows no magnetic ordering. A very strong

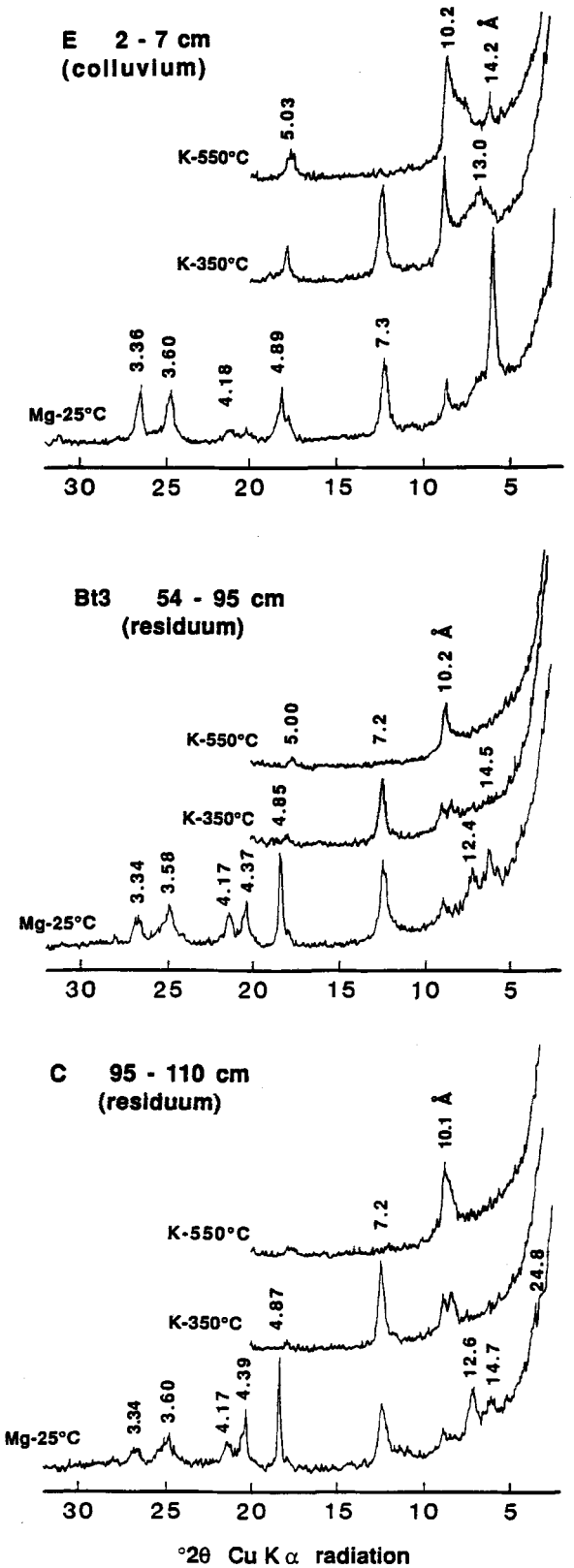

Figure 2. X-ray powder diffraction patterns for the <2-μm fractions of selected horizons from Pedon DU.

https://doi.org/10.1346/CCMN.1989.0370104 Published online by Cambridge University Press

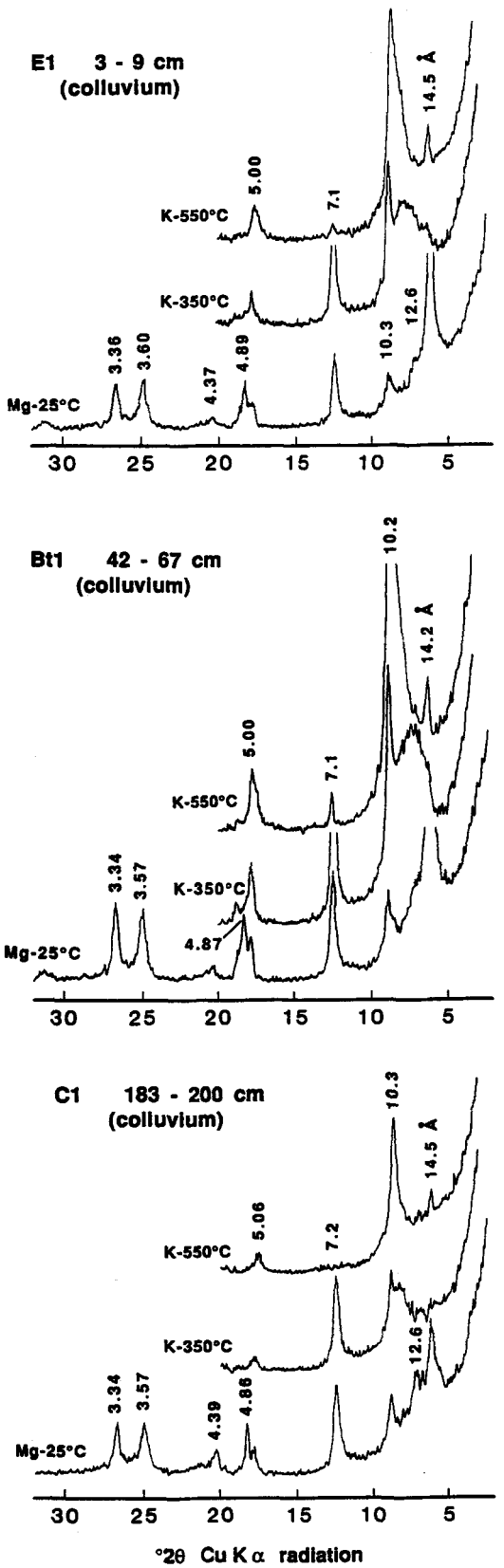

doublet exists with an isomer shift (IS) of 0.36 mm/s and quadrupole splitting (QS) of 0.63 mm/s due to the presence of Al-substituted goethite and other Fe^{3+}, presumably in silicates (Goodman, 1980). In addition, a small doublet, one peak of which is obscured is present, with IS = 1.13 mm/s and QS = 2.64 mm/s, attributable to Fe^{2+} in primary chlorite. The 77-K spectrum and its contributing components are plotted in Figure 4b. At this low temperature the Al-substituted goethite was magnetically ordered and produced a sextet with IS = 0.37 mm/s, QS = −0.20 mm/s, and a magnetic field (H) of 473 kOe. A strong Fe^{3+} doublet remained, at least partly due to Fe^{3+} in silicate structures, such as vermiculite. This doublet was also partly due to Al-substituted goethite particles so small that they did not order magnetically until even lower temperatures were imposed. The small doublet caused by Fe^{2+} in chlorite remained, although obscured in the 77-K spectrum. The Mössbauer spectra indicate that the clay fraction of the Pedon CF, Bt1 horizon contained a substantial amount of goethite and silicate-Fe^{3+}, as well as a small amount of Fe^{2+} in chlorite.

In contrast to the Pedon CF sample, the Pedon DU, Bt3 horizon clay fraction showed magnetic ordering at 298 K (Figure 4c). The resulting sextet was likely produced by hematite, with IS = 0.40 mm/s, QS = −0.20 mm/s, and H = 468 kOe, although this magnetic field was quite low for hematite (Goodman, 1980). A strong Fe^{3+} doublet was present, just as in the Pedon CF 298-K spectrum (Figure 4a), but no Fe^{2+} was detected. At 77 K (Figure 4d) the magnetic ordering of goethite was apparent, producing a sextet (IS = 0.36 mm/s, QS = −0.23 mm/s, H = 462 kOe) whose peaks were superimposed as inner shoulders on the peaks of the hematite sextet (IS = 0.36 mm/s, QS = −0.17 mm/s, H = 520 kOe). Again, an Fe^{3+} doublet persisted, although it was much smaller for this sample than for the Pedon CF sample. The data indicate that the clay fraction of the Pedon DU, Bt3 horizon contained substantial amounts of goethite and hematite, some Fe^{3+} in silicates, and no chlorite.

The fits shown in Figure 4 were adequate; however, they did not reproduce the asymmetric line shape of the goethite sextet in particular, which is caused by contributions from small particles having lower-than-average magnetic fields. Therefore, all 77-K spectra were fitted using a field distribution (Amarasiriwardena *et al.*, 1986). Two sextet distributions were assumed: goethite from 100 to 510 kOe in steps of 10 kOe and hematite from 510 to 550 kOe in steps of 5 kOe. In addition, an Fe^{3+} doublet distribution was assumed with QS from 0 to 1.4 mm/s in 0.1 mm/s

←

Figure 3. X-ray powder diffraction patterns for the <2-μm fractions of selected horizons from Pedon CF.

https://doi.org/10.1346/CCMN.1989.0370104 Published online by Cambridge University Press

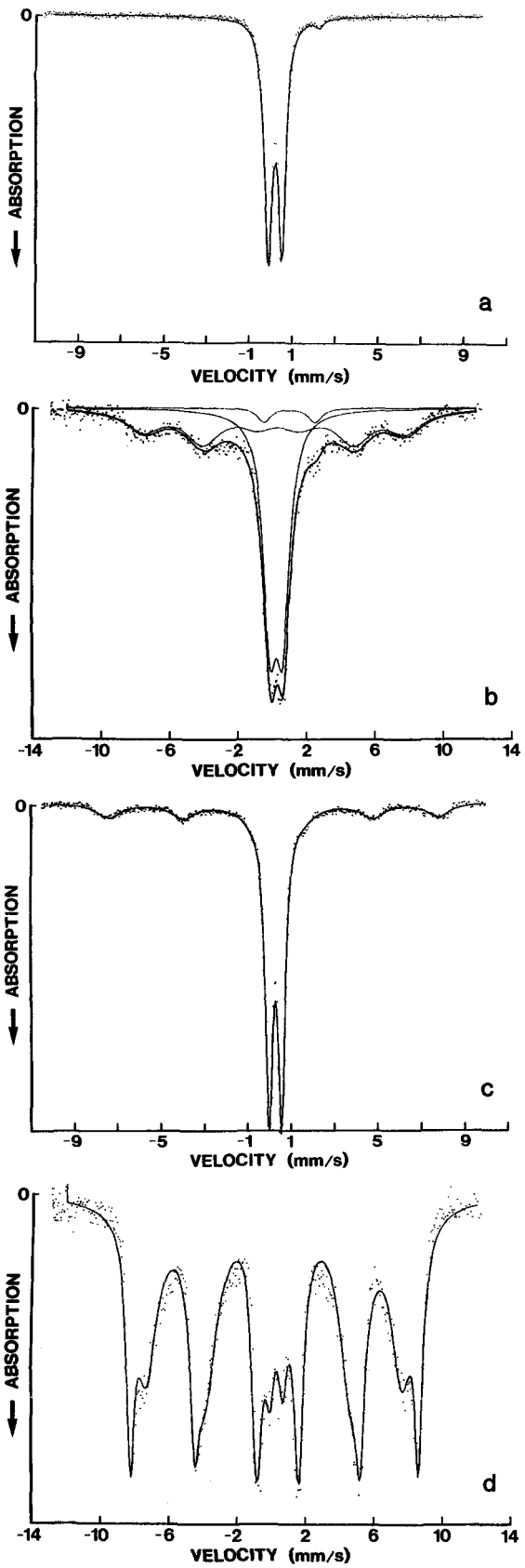

steps. When necessary, an Fe^{2+} doublet was also included in the fit, not distributed, but with variable QS and IS. The relative peak areas reported in Table 3 are from the distribution fits, which provide the most quantitative estimate for goethite-hematite ratios (Amarasiriwardena *et al.*, 1986). The other parameters, however, are from the simpler fits assuming one sextet each for goethite and hematite. Thus, the magnetic fields reported were compared directly with literature results on Al substitution.

Hematite. Typically, only one horizon from each pedon was analyzed by Mössbauer spectroscopy. Soil horizons derived from parent material containing almandine had much higher hematite contents and were redder than soils developed from almandine-free material (Table 4). Soil profile distribution of hematite was considered by using the complete data from Pedon DU, which had the strongest color differentiation of the soils analyzed (Table 4). The hematite content of the clay fraction increased with depth to the Bt3 horizon and decreased only slightly in the C horizon.

Estimates of Al substitution in hematite made from the observed Mössbauer magnetic fields were much greater than 15% (Table 4), which is the maximum expected (Schwertmann, 1985). These results indicate that the observed deviations from the magnetic field of pure hematite were due not only to Al substitution, but also to very small particle size ($\leq$100 Å) (Kündig *et al.*, 1966). Both factors reduce measured field values and are probably related, inasmuch as Al substitution results in smaller unit-cell size (Schwertmann, 1985). For two samples (Pedon CS, Bt2 and Pedon CL, Bt4), hematite was not observed in the 298-K spectra, but was detected by the 77-K analysis (Tables 2 and 3).

Goethite. Goethite was relatively abundant (13–22%) in all soil clays analyzed (Table 4). Higher clay-fraction goethite contents were found in residual soils than in colluvial soils, and goethite increased with depth in Pedon DU. Al substitution for Fe in goethite ranged from 15 to 33 atom %, which is the maximum reported for goethite (Schwertmann, 1985). The mole percent Al in dithionite extractable Fe oxides (which included both hematite and goethite) ranged from 9.5 to 17.1.

Other Fe^{3+} (the 77-K Fe^{3+} doublet). Of the soil clays analyzed, 8 to 45% of the total Fe was represented by an Fe^{3+} doublet at 77 K (Table 3). The nature of the Fe^{3+} doublet was further investigated by obtaining Mössbauer spectra at 40 K and 16 K, using a closed-cycle helium cryostat for cooling the absorber (Amarasiriwardena *et al.*, 1986) (see Figure 5, Table 5). A

←

Figure 4. Mössbauer spectra of representative soil clays. (a, b) Pedon CF, Bt1 horizon, 298 K and 77 K, respectively; (c, d) Pedon DU, Bt3 horizon, 298 K and 77 K, respectively.

https://doi.org/10.1346/CCMN.1989.0370104 Published online by Cambridge University Press

Table 2. Mössbauer data obtained at 298 K for soil clays.[1]

Pedon[2]	Horizon	Hematite W (mm/s)	Hematite H (kOe)	Hematite RA (%)	Fe^{3+} doublet QS (mm/s)	Fe^{3+} doublet RA (%)	Chlorite Fe^{2+} doublet IS (mm/s)	Chlorite Fe^{2+} doublet QS (mm/s)	Chlorite Fe^{2+} doublet RA (%)
DU	A	1.44	479	21	0.62	79	—	—	—
	E	1.07	479	20	0.62	78	1.10	2.61	2
	BA	1.36	480	23	0.60	77	—	—	—
	Bt1	1.41	471	20	0.59	80	—	—	—
	Bt2	1.17	478	20	0.59	80	—	—	—
	Bt3	1.25	468	27	0.58	73	—	—	—
	C	1.33	465	28	0.58	72	—	—	—
DE	Bw2	1.50	469	17	0.62	80	1.10	2.69	3
DH	Bw2	1.50	475	21	0.62	76	1.11	2.66	3
R	Bt2	1.40	487	17	0.59	83	—	—	—
CS	Bt2	—	—	—	0.59	100	—	—	—
CB	Bt2	—	—	—	0.60	97	1.16	2.59	3
CL	Bt2	—	—	—	0.60	97	1.13	2.59	3
	Bt4	—	—	—	0.54	100	—	—	—
CF	Bt1	—	—	—	0.63	97	1.13	2.64	3

[1] W is full width at half maximum for the outermost lines of the hematite sextet, H the average magnetic field, RA relative peak area, QS quadrupole splitting and IS isomer shift relative to metallic iron. Both hematite and Fe^{3+} doublet components had IS values (not quoted) of 0.36 ± 0.02 mm/s.

[2] Pedon identification symbols are keyed to geomorphic positions. See Table 1.

substantial portion of the 77-K doublet was in all samples due to poorly crystalline goethite, which becomes magnetically ordered at lower temperature. The field distribution for goethite also became narrower and more symmetric as the temperature was decreased (Figure 6). The doublet remaining at 16 K provided a good estimate of silicate Fe^{3+}. Comparing horizons A and C from Pedon DU (Table 5), silicate Fe^{3+} was prominent at the surface (18% relative area at 16 K) and became negligible in the C horizon.

A reduction in the Fe^{3+} 77-K doublet with temperature was also observed for the Pedon CS, Bt2 sample, which had 7% of its Fe in silicate form according to the results in Table 5. The hematite components in-

Table 3. Mössbauer data obtained at 77 K for soil clays.[1]

Pedon[2]	Horizon	Goethite W (mm/s)	Goethite H (kOe)	Goethite RA (%)	Hematite W (mm/s)	Hematite H (kOe)	Hematite RA (%)	Fe^{3+} doublet QS (mm/s)	Fe^{3+} doublet RA (%)	Chlorite Fe^{2+} doublet IS (mm/s)	Chlorite Fe^{2+} doublet QS (mm/s)	Chlorite Fe^{2+} doublet RA (%)
DU	A[3]	1.62	461	50	0.54	521	16	0.71	34	1.2	3.2	tr?
	E[3]	1.42	466	54	0.51	522	17	0.75	29	1.0	3.2	tr?
	BA	1.47	464	63	0.52	521	18	0.79	19	1.2	3.0	tr?
	Bt1	1.53	465	65	0.52	521	18	0.71	17	1.3	3.3	tr?
	Bt2	1.46	465	67	0.49	521	20	0.73	14	—	—	—
	Bt3	1.54	462	63	0.55	520	28	0.75	8	—	—	—
	C	1.55	462	67	0.52	519	25	0.80	8	—	—	—
DE	Bw2[3]	1.58	462	53	0.58	520	15	0.85	29	1.1	3.1	4
DH	Bw2[3]	1.89	458	46	0.68	519	14	0.76	36	1.1	3.1	4
R	Bt2	1.59	460	72	0.47	521	12	0.71	16	—	—	—
CS	Bt2	1.84	447	75	0.30*	518	7	0.74	18	—	—	—
CB	Bt2[3]	1.73	442	63	—	—	—	0.77	34	1.1	3.3	4
CL	Bt2[3]	2.27	448	56	—	—	—	0.73	40	1.1	3.1	4
	Bt4	2.02	464	69	0.30*	518	10	0.68	21	—	—	—
CF	Bt1[3]	2.41	473	51	—	—	—	0.74	45	1.1	3.0	4

[1] W is full width at half maximum for the outermost lines of the hematite sextet, H the average magnetic field, RA relative peak area, QS quadrupole splitting and IS isomer shift relative to metallic iron. All Fe^{3+} components had IS values (not shown) of 0.36 ± 0.02 mm/s. All RA values reported are obtained from analysis in terms of a distribution of fields (see text). In two cases, CS and CL Bt4, the small hematite component could only be seen in the distribution analysis and the width (0.30*) is the width of one component of the distribution.

[2] Pedon identification symbols are keyed to geomorphic positions. See Table 1.

[3] Colluvial soil material.

tr = trace; ? = questionable.

https://doi.org/10.1346/CCMN.1989.0370104 Published online by Cambridge University Press

Table 4. Color and Fe oxide characteristics of clay fractions (<2 μm) from selected soil horizons.

Pedon[2]	Horizon	Depth (cm)	Soil pH[3]	Dry clay		Goethite (%)	Hematite (%)	Al substitution (%)[1]			Fe_d (%)	Al_d (%)	Mole % Al in $Al_d + Fe_d$
				Munsell color	Redness rating[4]			Hematite 298 K	Hematite 77 K	Goethite 77 K			
DU	A[5]	0–2	4.4	10YR 6/4	0	13.3	3.8	24	28	22	11.0	2.0	15.4
	E[5]	2–7	4.3	10YR 5/4	0	16.5	4.7	24	26	19	13.6	2.1	13.5
	BA	7–20	4.7	7.5YR 6/6	2.5	17.1	4.4	24	28	20	13.8	2.1	13.4
	Bt1	20–34	4.9	7.5YR 5/6	3.0	18.5	4.6	28	28	20	14.8	2.0	12.0
	Bt2	34–54	5.2	5YR 5/6	6.0	19.6	5.3	25	28	20	16.0	2.0	11.2
	Bt3	54–95	5.6	5YR 5/8	8.0	19.9	7.9	29	31	21	18.0	2.1	10.3
	C	95–110	5.4	5YR 5/8	8.0	22.2	7.5	31	33	21	19.2	2.0	9.5
DE[6]	Bw2[5]	35–70	5.5	7.5YR 5/6	3.0	16.8	4.3	29	33	22	13.6	2.1	13.6
DH[6]	Bw2[5]	35–60	5.6	7.5YR 5/6	3.0	14.9	4.1	26	33	24	12.2	2.4	16.6
R[6]	Bt2	21–42	4.6	7.5YR 5/6	3.0	20.8	3.1	21	28	23	15.2	2.3	13.0
CS[6]	Bt2	32–53	4.5	8YR 5/6	2.4	19.3	1.6	—	36	30	13.2	2.2	14.3
CB	Bt2[5]	16–52	5.1	10YR 5/6	0	14.4	—	—	—	33	9.0	1.9	17.1
CL	Bt2[5]	32–65	5.5	10YR 5/6	0	13.4	—	—	—	29	8.4	1.7	17.1
	Bt4	85–105	5.5	7.5YR 6/8	3.33	14.2	1.9	—	36	20	10.2	1.6	13.2
CF	Bt1[5]	42–67	5.5	10YR 5/6	0	14.1	—	—	—	15	8.9	1.8	16.8

[1] Calculated from the Mössbauer magnetic field (H) values (DeGrave *et al.*, 1982; Golden *et al.*, 1979). 15% Al substitution in hematite is the maximum expected. High values suggest small particle size (≤100 Å).
[2] Pedon identification symbols are keyed to geomorphic positions. See Table 1.
[3] Soil pH determined in a 1:1 suspension of soil : water.
[4] Redness rating (RR) = (10 − YR hue) × (chroma) ÷ (value) (Torrent *et al.* 1983).
[5] Colluvial soil material.
[6] Soil derived from almandine-bearing parent rock.

dicated by these spectra were relatively constant with temperature, as was expected, inasmuch as hematite was usually magnetically ordered to room temperature.

The small amount of hematite in the Bt2 horizon of Pedon CS was not observed at 298 K (Table 2) nor in the low-temperature spectra when they were analyzed with a single sextet for goethite; however, the hematite shoulder on the goethite peaks was readily observed by field distribution analysis (Figure 7). The magnetic fields observed at 16 K were lower than those for pure hematite and goethite, as expected from the results at higher temperatures. The magnetic fields for goethite at 16 K were too low compared to the prediction from the Al substitutions in Table 4 (using equations reported by Bowen and Weed, 1984). The magnetic fields for hematite should be saturated at 77 K and not change as the temperature is lowered; however, a distinct increase was observed in all samples measured at 16 K. Both these observations are consistent with poor crystallinity contributing to the observed fields even at low temperature.

Chlorite. Chlorite Fe^{2+} was observed unambiguously in the clay fractions of Pedons DE, DH, CB, CF, and CL (Bt2). It was also a possible minor component in the upper horizons of Pedon DU (labeled tr? in Table 3), because analysis of the 77-K spectra of these samples including about 2% of this component gave some-

Table 5. Mössbauer data obtained at low temperature for selected clays.[1]

Pedon[2]	Horizon	T (K)	Goethite W (mm/s)	Goethite H (kOe)	Goethite RA (%)	Hematite W (mm/s)	Hematite H (kOe)	Hematite RA (%)	Fe^{3+} doublet QS (mm/s)	Fe^{3+} doublet RA (%)
DU	A	40	1.31	477	56	0.34	523	17	0.76	27
		16	1.09	484	62	0.32	526	20	0.79	18
DU	C	40	1.18	478	73	0.34	523	24	0.83	3
		16	0.94	488	71	0.32	528	28	0.83	1
CS	Bt2	40	1.44	463	87	0.27[3]	521	5	0.73	8
		16	0.96	480	86	0.27[3]	524	7	0.69	7

[1] W is full width at half maximum for the outermost lines of the hematite and goethite sextets, H the average magnetic field, RA relative peak area, QS quadrupole splitting. All RA values reported are obtained from analysis in terms of a distribution of fields (see text). In the case of Pedon CS, Bt2 horizon, the small hematite component could only be seen in the distribution analysis.
[2] Pedon identification symbols are keyed to geomorphic positions. See Table 1.
[3] Width of one component of the distribution.

https://doi.org/10.1346/CCMN.1989.0370104 Published online by Cambridge University Press

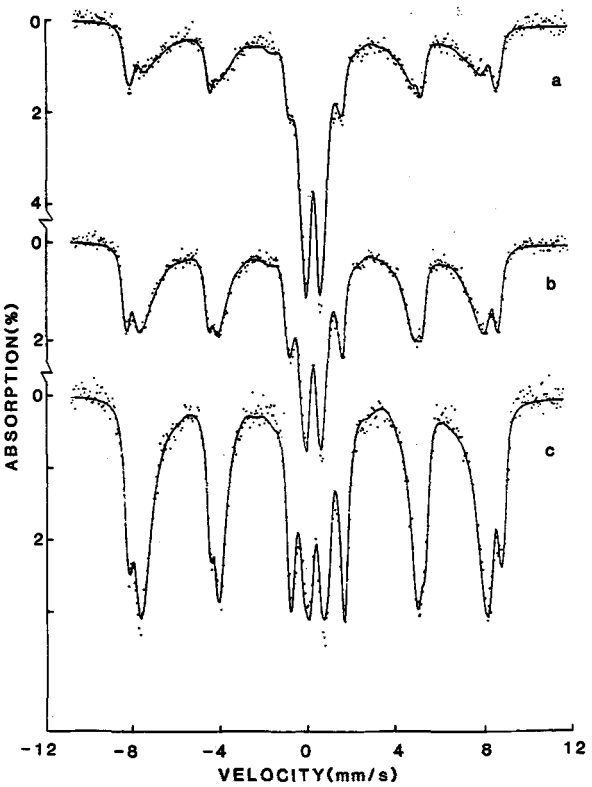

Figure 5. Mössbauer spectra of clay fraction of Pedon DU, A horizon, fitted with two distributions of hyperfine fields and a quadrupole distribution. (a) at 80 K, (b) at 40 K, and (c) at 16 K.

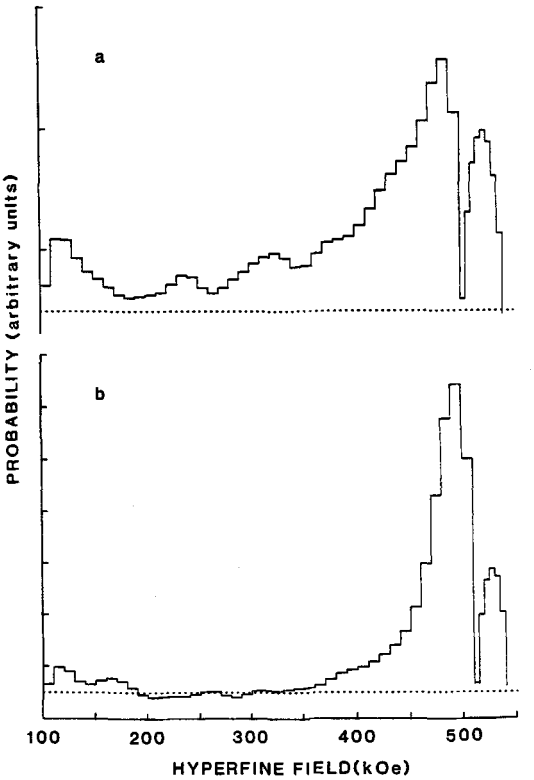

Figure 6. Probability distributions of hyperfine fields for Pedon DU A horizon clay. (a) at 80 K, (b) at 16 K.

what improved fits. At 298 K, only the E horizon sample of Pedon DU had a spectrum improved by the inclusion of Fe^{2+} (Table 2). The 40-K and 16-K spectra of the Pedon DU, A horizon sample showed no evidence of Fe^{2+} (Table 5), but peak overlap could have obscured a small amount.

DISCUSSION

Phyllosilicates

As indicated by the XRD data in Figures 1–3, the clay fractions of soil horizons developed in colluvium contained a larger proportion of 2:1 phyllosilicates and chlorite than the clay fractions from residual soil horizons and saprolite. Because colluvium has been transported, it has been physically, as well as chemically, weathered. In contrast, saprolite and soil residuum have essentially been only chemically weathered *in situ.* Abrasion during colluvial transport appears to have facilitated the mechanical breakdown of micas, vermiculite, hydroxy-interlayer vermiculite (HIV), and chlorite into the clay fraction of colluvial soil horizons.

Vermiculite and HIV. Graham *et al.* (1989) found vermiculite to be a weathering product of sand-size biotite from the saprolite of Pedon CL (same soil as in this study). Although small amounts were present in the clay fraction of saprolite and soil residuum (Figures 1 and 2), vermiculite became a dominant component of the clay fraction of colluvial soil horizons (Figures 1–3). The transformation of biotite to vermiculite probably occurred chiefly in sand and silt fractions inasmuch as only relatively small XRD peaks for mica were found throughout the clay fractions. This vermiculite (as well as HIV) must have contained most of the silicate Fe^{3+} detected by Mössbauer spectroscopy (Fe^{3+} doublet at 16 K, Table 5). In a study of biotite weathering, Goodman and Wilson (1973) also found vermiculite to contain Fe^{3+}, which increased relative to Fe^{2+} from the C to the A horizon of a soil in Scotland. In the present study, the increase in silicate Fe^{3+} in the A horizon of Pedon DU compared to the C horizon (Table 5) was likely due to the comminution of vermiculite into the clay fraction in the colluvial surface horizon.

HIV is common in soils of the southeastern United States (Barnhisel, 1978) and has been reported in soils of the southern Blue Ridge (Losche *et al.,* 1970; Rebertus and Buol, 1985). The formation of HIV has been attributed to the hydrolysis and polymerization of Al^{3+} in vermiculite interlayers in acid soils (Barnhisel, 1977). In the present study, hydroxy-interlayering of vermiculite was found to be insignificant or nonexistent in

https://doi.org/10.1346/CCMN.1989.0370104 Published online by Cambridge University Press

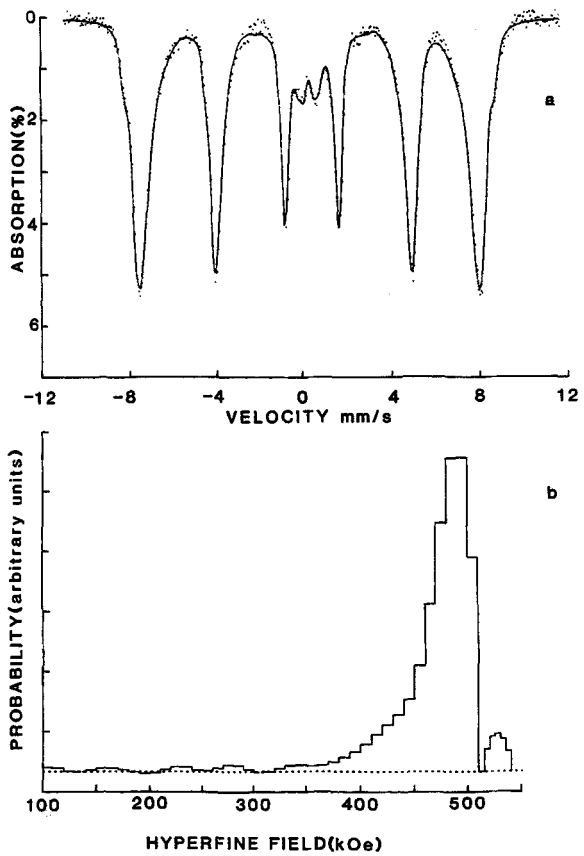

Figure 7. For Pedon CS, Bt2 horizon clay at 16 K: (a) Mössbauer spectrum fitted with two distributions of hyperfine fields and a quadrupole distribution. (b) Probability distribution of hyperfine fields. Note hematite peak above 510 kOe.

saprolite and in residual C horizons (e.g., Figures 1 and 2), but interlayering was evident in all surface horizons and throughout colluvial soils, even in their C horizons (Figures 1–3). The HIV in colluvial C horizons may have formed in acid surface-soil horizons, the material of which was subsequently transported and deposited downslope. As pointed out by Graham *et al.* (1989) in a study of the sand fractions of these same soils, the genetic interpretation of mineral weathering in colluvial soils is often uncertain.

Chlorite. The presence of primary chlorite in these soil clays is noteworthy, inasmuch as chlorite is generally perceived to be unstable in soil environments (Allen and Fanning, 1983). Mössbauer spectroscopy detected more chlorite (as indicated by the relative area of the Fe^{2+} doublet) in colluvial soil horizons, which had been subject to both physical and chemical weathering, than in residual soil horizons, which had experienced primarily chemical weathering (Table 3). Comminution of sand-size primary chlorite reduced this mineral to the clay fraction, where it persists, apparently unaltered, even in the surface horizons (14-Å peak after heating sample to 550°C, Figures 1–3), where weathering has probably been most intense. Chlorite appears to have been more stable in these soils than biotite, which altered to secondary minerals in all size fractions. Neither interstratified chlorite/vermiculite, a common weathering product of chlorite (Herbillon and Makumbi, 1975; Rabenhorst *et al.*, 1982; Rice *et al.*, 1985), nor any other weathering products of chlorite were identified. The freshness of the chlorite was probably due to the lack of intensive weathering in these mountain soils. Bain (1977) reported that Fe^{2+}-chlorite persists in the clay fraction with very little alteration in all horizons of weakly developed, till-derived soils in Scotland. It is in more intensely weathered soils, such as those in Zaire (Herbillon and Makumbi, 1975) and the Piedmont of the eastern United States (Rabenhorst *et al.*, 1982; Rice *et al.*, 1985), that chlorite alteration has been documented.

Kaolinite. Graham *et al.* (1989) found kaolinite as a pseudomorphic alteration product of sand-size biotite in the same soils examined in the present study. Comminution of these weathered biotite grains released kaolinite into the clay fraction of the soils. This mechanism was invoked previously by Wilson (1967) in a study of clay mineralogy of soils derived from biotite-rich quartz gabbro in Scotland, and by Rebertus *et al.* (1986) in a study of biotite kaolinization in soils and saprolite derived from mica gneiss and mica schist in North Carolina.

Oxides and oxyhydroxides

Gibbsite. The weathering of aluminosilicate minerals, primarily plagioclase, biotite, and almandine (Graham *et al.*, 1989), released Si and Al into solution in the soils and saprolite. Si was depleted in these materials because it is relatively soluble under all common soil pH conditions, but Al has a very low solubility between pH 5 and 8 (Keller, 1964). Because the pH in the C and Cr horizons of these soils was typically between 5 and 6 (Graham, 1986), Al precipitation as gibbsite was favored in those horizons. Probably both the Al released by weathering within the C and Cr horizons and the Al leached from the more acid weathering environments of the surface horizons precipitated as gibbsite in these lower horizons. As a result, gibbsite was found to be most abundant in the clay fraction of residual C and Cr horizons and to decrease toward the surface (Figures 1 and 2). Other factors which may have contributed to this decrease include: (1) dilution caused by comminution of phyllosilicates into the clay fraction; (2) preferential illuviation of the very small gibbsite particles; (3) competition for Al ions by HIV and complexation of Al by organic acids, thus preventing further gibbsite precipitation; and (4) resilication of gibbsite, although evidence for this mechanism is not immediately obvious. The trend of decreasing gibbsite

https://doi.org/10.1346/CCMN.1989.0370104 Published online by Cambridge University Press

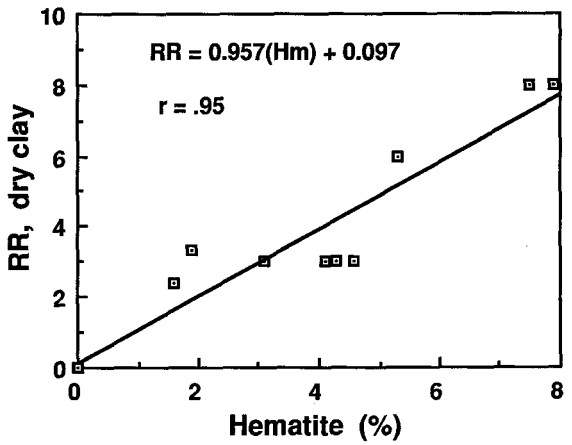

Figure 8. Relationship between redness rating (RR) (Torrent *et al.*, 1983) and hematite content of clay fractions (<2 μm).

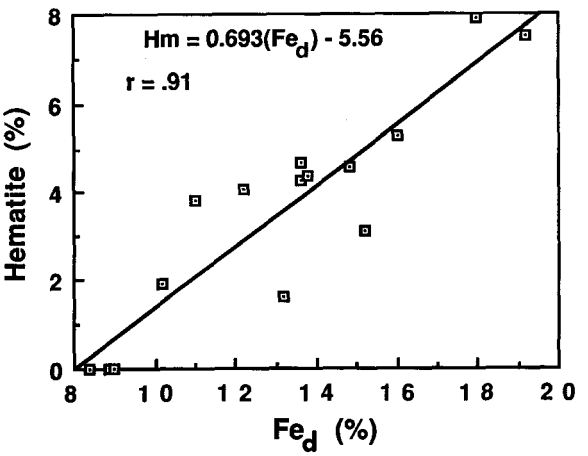

Figure 9. Relationship between hematite and dithionite-extractable iron (Fe_d) contents of clay fractions (<2 μm).

toward the surface was less evident in colluvial soils (see, e.g., Figure 3), possibly because the colluvial deposits had relatively homogeneous depth distributions of weathered minerals which had already been depleted of Al and were therefore no longer sources for further gibbsite production. Also, some colluvial deposits may not have been in place long enough for the pedogenic differentiation of gibbsite distributions. In any case, gibbsite comprises a much lower proportion of the clay fraction throughout colluvial soils (Figure 3) than in soil horizons developed in residuum (Figures 1 and 2).

Hematite. The occurrence of hematite in these soils is strongly dependent on the parent rock mineralogy. Soils derived from almandine-bearing parent materials had higher hematite contents than those developed in material without almandine (Table 4). Graham *et al.* (1989) examined the weathering of Fe-bearing primary minerals in the same soils and saprolites examined in the present study and found hematite only in association with weathered almandine grains.

The increase in hematite content with depth in Pedon DU (Table 4) was probably influenced by several factors. First, the subsoil immediately above the saprolite is where much Fe was oxidized and released from primary minerals, such as almandine. This flush of Fe probably exceeded the solubility constant for ferrihydrite, at least in microenvironments. The precipitated ferrihydrite, a necessary hematite precursor, was dehydrated and structurally rearranged to yield hematite (Schwertmann and Taylor, 1977). Second, the high organic matter content of the surface horizons was antagonistic to hematite formation and may have promoted its dissolution (Schwertmann, 1985). Third, because of its extremely small particle size, hematite may have been preferentially illuviated, resulting in its concentration with depth.

Coinciding with the increase in hematite content in Pedon DU are increasingly redder dry clay hues (Table 4). Finely divided hematite, as it occurs in soils, is a very effective red pigmenting agent (Schwertmann and Taylor, 1977), and soil redness has been correlated with hematite content by using a "redness rating" (Torrent *et al.*, 1983). This redness rating (RR) is defined in terms of the Munsell color parameters, RR = (10 − YR hue) × (chroma) ÷ (value). A strong correlation between hematite content and RR was found in the present study using dry clay colors (r = .95, Figure 8). Soils containing >1% organic carbon were excluded from the correlations because the carbon interferes with the expression of redness. Despite sodium hypochlorite pretreatment of the soils, apparently sufficient organic carbon remained in the clays to mask redness.

Colluvial soils, particularly Pedons DE and DH, had quite uniform soil colors. Only one horizon from each of these pedons was analyzed with Mössbauer spectroscopy. These horizons were both the same color and had similar hematite contents (Table 4). The uniformity of soil color and hematite content in colluvial soils probably resulted from the homogenization of preweathered soil material during colluvial transport. A similar effect was noted by Torrent *et al.* (1980), who found that soils formed in preweathered alluvium showed no further pedogenic differentiation of Fe-oxides despite terrace level (age).

Although soil color is not solely dependent on dithionite-extractable iron oxide content (Fe_d) (Bigham *et al.*, 1978), a strong correspondence existed between redness and Fe_d for the soil clays examined here (Table 4). This correspondence was due to the fact that hematite content, the cause of the redness, increased with increasing clay fraction Fe_d in these soils (r = .91; Figure 9). Apparently, conditions that favored the accumulation of Fe oxides in these soils also favored hematite formation. Such conditions include the presence

of easily weathered mafic minerals, which readily release high concentrations of Fe, and illuvial horizons in which translocated Fe oxides, including hematite, may have accumulated.

Goethite. Graham *et al.* (1989) found goethite, in addition to hematite, as a weathering product of almandine in these same soils. Goethite, however, was found in the clay fraction of all soils (Table 4), whether or not they were derived from almandine-bearing rocks; thus, almandine weathering was not the sole means of goethite formation. In a study of biotite weathering in Australia, Banfield and Eggleton (1988) found goethite crystallized within individual partially kaolinized biotite grains. The goethite was detected with high-resolution transmission electron microscopy and selected-area electron diffraction, but XRD peaks for goethite were broad and poorly defined. In the present study, biotite was found to be an abundant Fe-bearing primary mineral in the parent rocks and to be relatively easily weathered; but XRD did not detect goethite coexisting with weathered biotite sand grains from the soil or saprolite (Graham *et al.,* 1989). The alteration of the biotite to kaolinite, described by Graham *et al.* (1989), must have released much Fe; however, the structural Fe of biotite was probably released in relatively low concentrations which, according to Schwertmann (1985), should have favored goethite formation, because the solution concentration of Fe would have exceeded the solubility product of goethite ($\sim 10^{-42}$), but not that of ferrihydrite ($\sim 10^{-37}$–10^{-39}), the necessary precursor of hematite.

The goethite content of the clay fraction increased with depth in Pedon DU (Table 4). This concentration of goethite may have been the result of illuviation, precipitation of organically chelated Fe carried in solution, or immediate precipitation of Fe released by primary mineral weathering. Goethite contents were also higher in the residual soil horizons than in colluvial horizons, probably reflecting greater pedogenic differentiation in the more stable residual soils.

Goethite imparts a yellowish-brown color to soils, but this is overridden by the red pigmentation of even very small amounts of hematite (Schwertmann and Taylor, 1977). In the present study, the pigmenting effect of goethite was evident only in the absence of hematite (Table 4). Because hematite in these soils was largely a product of almandine weathering, only those subsoil horizons developed in almandine-free parent material exhibited the yellow-brown coloration (10YR hues) of goethite (Table 4). All surface horizons had 10YR hues due to the influence of organic matter.

REFERENCES

Allen, B. L. and Fanning, D. S. (1983) Composition and soil genesis: in *Pedogenesis and Soil Taxonomy. I. Concepts and Interactions,* L. P. Wilding, N. E. Smeck, and G. F. Hall, eds., Elsevier, New York, 141–192.

Amarasiriwardena, D. D., DeGrave, E., Bowen, L. H., and Weed, S. B. (1986) Quantitative determination of aluminum-substituted goethite-hematite mixtures by Mössbauer spectroscopy: *Clays & Clay Minerals* **34,** 250–256.

Anderson, J. U. (1963) An improved pretreatment for mineralogical analysis of samples containing organic matter: in *Clays and Clay Minerals, Proc. 10th Natl. Conf., Austin, Texas, 1961,* A. Swineford and P. C. Franks, eds., Pergamon Press, New York, 380–388.

Bain, D. C. (1977) The weathering of chlorite minerals in some Scottish soils: *J. Soil Sci.* **28,** 144–164.

Banfield, J. F. and Eggleton, R. A. (1988) Transmission electron microscope study of biotite weathering: *Clays & Clay Minerals* **36,** 47–60.

Barnhisel, R. I. (1977) Chlorites and hydroxy interlayered vermiculite and smectite: in *Minerals in Soil Environments,* J. B. Dixon and S. B. Weed, eds., Soil Science Society of America, Madison, Wisconsin, 331–356.

Barnhisel, R. I., ed. (1978) Analyses of clay, silt and sand fractions of selected soils from southeastern United States: *Univ. Kentucky Agric. Exp. Sta., Southern Cooperative Bull.* **219,** 90 pp.

Bigham, J. M., Golden, D. C., Buol, S. W., Weed, S. B., and Bowen, L. H. (1978) Iron oxide mineralogy of well-drained Ultisols and Oxisols: II. Influence on color, surface area, and phosphate retention: *Soil Sci. Soc. Amer. J.* **42,** 825–830.

Bowen, L. H. and Weed, S. B. (1984) Mössbauer spectroscopy of soils and sediments: in *Chemical Mössbauer Spectroscopy,* R. H. Herber, ed., Plenum, New York, 217–242.

Calvert, C. S., Buol, S. W., and Weed, S. B. (1980) Mineralogical characteristics and transformations of a rock-saprolite-soil profile in the North Carolina Piedmont: II. Feldspar alteration products—Their transformations through the profile: *Soil Sci. Soc. Amer. J.* **44,** 1104–1112.

Churchman, G. J., Whitton, J. S., Claridge, G. G. C., and Theng, B. K. G. (1984) Intercalation method using formamide for differentiating halloysite from kaolinite: *Clays & Clay Minerals* **32,** 241–248.

Coffin, D. E. (1963) A method for the determination of free iron in soils and clays: *Can. J. Soil Sci.* **43,** 7–17.

DeGrave, E., Bowen, L. H., and Weed, S. B. (1982) Mössbauer study of aluminum-substituted hematites: *J. Mag. Mag. Mat.* **27,** 98–108.

Fanning, D. S. and Keramidas, V. Z. (1977) Micas: in *Minerals in Soil Environments,* J. B. Dixon and S. B. Weed, eds., Soil Science Society of America, Madison, Wisconsin, 195–258.

Golden, D. C., Bowen, L. H., Weed, S. B., and Bigham, J. M. (1979) Mössbauer studies of synthetic and soil-occurring aluminum substituted goethite: *Soil Sci. Soc. Amer. J.* **43,** 802–808.

Goodman, B. A. (1980) Mössbauer spectroscopy: in *Advanced Chemical Methods for Soil and Clay Minerals Research,* J. W. Stucki and W. L. Banawart, eds., D. Reidel, Dordrecht, 1–92.

Goodman, B. A. and Wilson, M. J. (1973) A study of the weathering of a biotite using the Mössbauer effect: *Mineral. Mag.* **39,** 448–454.

Graham, R. C. (1986) Geomorphology, mineral weathering, and pedology in an area of the Blue Ridge Front, North Carolina: Ph.D. dissertation, North Carolina State University, Raleigh, North Carolina, 196 pp.

Graham, R. C., Weed, S. B., Bowen, L. H., and Buol, S. W. (1989) Weathering of iron-bearing minerals in soils and saprolite on the North Carolina Blue Ridge Front: I. Sand-size primary minerals: *Clays & Clay Minerals* **37,** 19–28.

Harris, W. G., Zelazny, L. W., and Bloss, F. D. (1985) Biotite

kaolinization in Virginia Piedmont soils: II. Zonation in single grains: *Soil Sci. Soc. Amer. J.* **49,** 1297–1302.

Herbillon, A. J. and Makumbi, M. H. (1975) Weathering of chlorite in a soil derived from a chlorite-schist under humid tropical conditions: *Geoderma* **13,** 89–104.

Jackson, M. L. (1979) *Soil Chemical Analysis—Advanced Course:* 2nd ed., 11th printing, Publ. by author, Madison, Wisconsin, 895 pp.

Keller, W. D. (1964) The origin of high alumina clay minerals. A review: in *Clays and Clay Minerals, Proc. 12th Natl. Conf., Atlanta, Georgia, 1963,* W. F. Bradley, ed., Pergamon Press, New York, 129–156.

Kündig, W., Bömmel, H., Constabaris, G., and Lindquist, R. H. (1966) Some properties of supported small α-Fe_2O_3 particles determined with the Mössbauer effect: *Phys. Rev.* **142,** 327–333.

Losche, C. K., McCracken, R. J., and Davey, C. B. (1970) Soils of steeply sloping landscapes in the southern Appalachian Mountains: *Soil Sci. Soc. Amer. Proc.* **34,** 473–478.

Rabenhorst, M. C., Fanning, D. S., and Foss, J. E. (1982) Regularly interstratifiifed chlorite/vermiculite in soils over meta-igneous mafic rocks in Maryland: *Clays & Clay Minerals* **30,** 156–158.

Rebertus, R. A. and Buol, S. W. (1985) Iron distribution in a developmental sequence of soils from mica gneiss and schist: *Soil Sci. Soc. Amer. J.* **49,** 713–720.

Rebertus, R. A., Weed, S. B., and Buol, S. W. (1986) Transformations of biotite to kaolinite during saprolite-soil weathering: *Soil Sci. Soc. Amer. J.* **50,** 810–819.

Rice, T. J., Jr., Buol, S. W., and Weed, S. B. (1985) Soil-saprolite profiles derived from mafic rocks in the North Carolina Piedmont: I. Chemical, morphological and mineralogical characteristics and transformations: *Soil Sci. Soc. Amer. J.* **49,** 171–178.

Sawhney, B. L. (1977) Interstratification in layer silicates: in *Minerals in Soil Environments,* J. B. Dixon and S. B. Weed, eds., Soil Science Society of America, Madison, Wisconsin, 405–434.

Schwertmann, U. (1985) The effect of pedogenic environments on iron oxide minerals: in *Advances in Soil Science, Vol. 1,* B. A. Stewart, ed., Springer-Verlag, New York, 171–200.

Schwertmann, U. and Taylor, R. M. (1977) Iron oxides: in *Minerals in Soil Environments,* J. B. Dixon and S. B. Weed, eds., Soil Science Society of America, Madison, Wisconsin, 145–180.

Theisen, A. A. and Harward, M. E. (1962) A paste method for preparation of slides for clay mineral identification by X-ray diffraction: *Soil Sci. Soc. Amer. Proc.* **26,** 90–91.

Torrent, J., Schwertmann, U., Fechter, H., and Alferez, F. (1983) Quantitative relationships between soil color and hematite content: *Soil Sci.* **136,** 354–358.

Torrent, J., Schwertmann, U., and Schulze, D. G. (1980) Iron oxide mineralogy of some soils of two river terrace sequences in Spain: *Geoderma* **23,** 191–208.

Wilson, M. J. (1967) The clay mineralogy of some soils derived from a biotite-rich quartz-gabbro in the Strathdon area, Aberdeenshire: *Clay Miner.* **7,** 91–100.

(Received 26 October 1987; accepted 21 June 1988; Ms. 1723)